Research Article

ADVANCED PHOTONICS

Generation of fractional spatiotemporal optical vortices and anomalous topological conservation in the second harmonic

Dawei Liu,[a,†] Xingyuan Zhang,[a,b,†] Daijun Luo,[a,c] Huiming Wang,[d] Zhirong Tao,[e] Dana JiaShaner,[a] Guangyu Fan,[a,*] and Qiwen Zhan[a,b,f]

[a]University of Shanghai for Science and Technology, School of Optical-Electrical and Computer Engineering, Shanghai, China
[b]Westlake University, School of Engineering, Zhejiang Key Laboratory of 3D Micro/Nano Fabrication and Characterization, Department of Electronic and Information Engineering, Hangzhou, China
[c]King's College London, Department of Physics, Attosecond Quantum Physics Laboratory, London, United Kingdom
[d]TU Wien, Institute of Photonics, Vienna, Austria
[e]Karlsruhe Institute of Technology, Karlsruhe, Germany
[f]Hiroshima University, International Institute for Sustainability with Knotted Chiral Meta Matter (WPI-SKCM2), Higashihiroshima, Japan

Abstract. Spatiotemporal optical vortices (STOVs), which carry transverse orbital angular momentum on ultrafast timescales, provide a platform to probe intrinsic space–time coupling in light–matter interactions. Fractional-order STOVs (FSTOVs) introduce continuously tunable topology, giving access to controllable orientation and chirality, but their noninteger winding breaks single-valuedness and global topological protection, so their generation and nonlinear response have remained unclear. Here, we investigate the topological dynamics of FSTOVs and demonstrate anomalous angular-momentum conservation in second-harmonic generation (SHG). As the fractional charge increases, the field evolves from an open to a closed structure, with singularities migrating inward and reorganizing. Although SHG preserves global phase doubling, the singularities do not follow the simple 2ℓ rule but undergo local multiplication and reorganization into spatiotemporal interference networks. This coexistence of global conservation and local reconstruction defines a framework for nonlinear topological dynamics of structured light and enables ultrafast field control and topological information transfer.

Keywords: orbital angular momentum; spatiotemporal optical vortices; fractional-order vortices.

Received Nov. 18, 2025; revised manuscript received Feb. 19, 2026; accepted for publication Apr. 22, 2026; published online May 25, 2026.

[DOI: 10.1117/1.AP.8.3.036017]

1 Introduction

The angular momentum of light provides a fundamental degree of freedom for controlling and utilizing electromagnetic fields. Since their discovery, optical vortices carrying orbital angular momentum (OAM) have become a cornerstone of structured light research, driving transformative advances in optical manipulation, high-resolution imaging, communication, and quantum photonics.[1–7] Conventional vortex beams possess longitudinal OAM along the propagation axis, with a phase singularity embedded in space, forming a characteristic ring-shaped intensity profile with a central dark core.[8–10] Recently, this concept has been extended into the spatiotemporal domain, giving rise to spatiotemporal optical vortices (STOVs). In STOVs, the helical phase is distributed on the space–time plane, leading to transverse OAM orthogonal to the propagation direction.[11–14] The emergence of STOVs expands the dimensionality of optical topology and reveals strong coupling between energy flow and phase structure.[15–19] These unique couplings make STOVs ideal for studying ultrafast light–matter interactions, nonlinear dynamics, and high-dimensional information transport. Importantly, angular momentum conservation in nonlinear frequency conversion and high-harmonic generation (HHG) has been a central

*Address all correspondence to Guangyu Fan, gfan@usst.edu.cn
†These authors contributed equally to this work.

principle in vortex optics, where integer-order STOVs have been shown to preserve their OAM through phase doubling in harmonic fields.[20–22]

In the spatial domain, fractional orbital angular momentum (fractional OAM) has long served as a bridge between integer topological states.[23–28] Its noninteger phase winding breaks global 2π closure and introduces a branch cut that preserves field continuity. This nonclosed phase provides the field with directionality and chirality while simultaneously breaking single-valuedness and topological protection. Fractional OAM beams thus offer a rich platform for studying continuous topological transitions and singularity dynamics in structured light.[29–31] Beyond fundamental physics, the high dimensionality of fractional OAM provides substantial potential for high-capacity optical communication and information multiplexing, as recently demonstrated by deep-learning-assisted recognition and transmission of fractional OAM modes.[32] However, previous studies have been confined to the spatial domain, and no spatiotemporal fractional vortices have yet been realized. More importantly, it remains unclear whether the topological conservation established for integer-order STOVs in nonlinear frequency conversion, characterized by phase doubling and OAM scaling, still holds for fractional states.

In this work, we experimentally generate and systematically characterize fractional-order spatiotemporal optical vortices (FSTOVs) and uncover their anomalous topological conservation during second-harmonic generation (SHG). We reveal that the continuous variation of the fractional topological charge induces a redistribution of temporal energy flow, driving the transition of the intensity structure from an open to a closed configuration and accompanied by the inward migration of phase singularities. More importantly, we demonstrate that although the global phase in SHG obeys a strict doubling, the local singularity network does not follow the simple 2ℓ rule, exhibiting a reorganization and multiplication of topological defects instead. This anomalous topological behavior originates from mode-dependent coherent superposition in FSTOVs, resulting in the coexistence of global OAM conservation and local topological reconstruction. Our findings establish FSTOVs as a new class of nontrivial spatiotemporal topological states that combine coherent superposition with nonlinear transformation. The demonstrated control of singularity geometry and chirality reveals a deeper mechanism linking nonlinearity and topology in structured light. By showing that global conservation can coexist with local reconstruction, this work establishes a new paradigm for understanding how nonlinear interactions reshape the topological order in complex optical fields. These insights extend the foundations of optical topology beyond the linear regime and open avenues toward high-dimensional information encoding, ultrafast topological photonics, and the broader study of symmetry breaking in nonlinear light–matter interactions.

2 Results

2.1 Generation and Evolution Dynamics of FSTOVs

Unlike integer-order STOVs, a fractional-order STOV (FSTOV) possesses a noninteger topological charge, preventing the phase from completing a full 2π rotation along any closed path. This breaks the single-valued nature of the field and introduces a branch cut—a radial phase discontinuity that originates from the beam center and extends outward. Mathematically, a fractional azimuthal phase $\exp(i\ell\varphi)$ with noninteger ℓ is intrinsically multivalued, so a branch cut must be introduced along a chosen radial direction, across which the phase undergoes a discontinuous jump of $2\pi\delta$, with $\ell = m + \delta$ ($m \in \mathbb{Z}$, $\delta \neq 0$). Physically, this branch cut stores the fractional circulation of the field; however, as only integer-charge vortices are topologically stable under free-space propagation, such a continuous fractional singularity is unstable and typically resolves into discrete integer-charge (usually unit-charge) vortices distributed along or near the original cut, thereby restoring local single-valuedness through a redistribution of the topological charge. In intensity, this discontinuity manifests as an open gap on the otherwise ring-shaped profile, signifying the loss of rotational symmetry and the breakdown of global topological protection. As illustrated schematically in Fig. 1(a), such a fractional state can be interpreted as a coherent superposition of two neighboring integer-order STOV modes. The interference between these modes produces a continuous transition of the phase helicity between adjacent topological orders, yielding the characteristic open-ring intensity and the branch-like phase discontinuity of an FSTOV.

As shown in Fig. 1(b), for $\ell = 0.2$, the beam exhibits an arc-shaped intensity profile with a bright asymmetric ring surrounding a dark core. The phase remains nearly flat near the open gap, where no clear singularity is formed. When ℓ increases to 0.4, a local phase zero first appears at the outer edge, aligned with the gap direction. As ℓ further increases, the intensity redistributes, and the gap gradually closes while the singularity moves inward toward the beam center, forming a characteristic "gap-healing and inward-migration" process. At $\ell \approx 0.8$, the two ends nearly connect, leaving only a faint low-intensity region. When $\ell = 1$, the gap disappears, the ring symmetry is restored, and the phase winds exactly 2π, recovering the integer vortex state.

Physically, an FSTOV with topological charge $\ell = m + \delta$ (where $m \in \mathbb{Z}$ and $\delta \in [0,1)$) is modeled as a coherent superposition of two adjacent integer Laguerre-Gaussian modes E_k (Sec. 1 in the Supplementary Material):

$$E_{\mathrm{FSTOV}}(\rho,\phi) \approx C_m(\ell)E_m(\rho,\phi) + C_{m+1}(\ell)E_{m+1}(\rho,\phi), \tag{1}$$

where the coefficients are $C_k(\ell) = e^{i\pi(\ell-k)}\mathrm{sinc}[\pi(\ell-k)]$.[23] The destructive interference between these modes induces a phase singularity at a radial position ρ^*, determined by

$$\rho^*(\delta) = \frac{w_0}{\sqrt{2}}\sqrt{m+1}\,\frac{1-\delta}{\delta}. \tag{2}$$

This relation governs the topological reconstruction relative to the beam waist w_0. As δ evolves from 0 to 1, the singularity migrates continuously from the periphery ($\lim_{\delta\to 0}\rho^* \to \infty$) inward, eventually merging with the central vortex at the limit $\lim_{\delta\to 1}\rho^* \to 0$.

2.2 Orientation and Chirality Properties of FSTOVs

For conventional integer-order STOVs, the phase winds by an exact 2π around any closed loop, ensuring rotational symmetry of the field.[15,18] In such cases, changing the initial phase orientation does not alter the spatiotemporal intensity profile. By contrast, fractional STOVs depart from this symmetry. The presence of a branch-like phase discontinuity breaks the global 2π

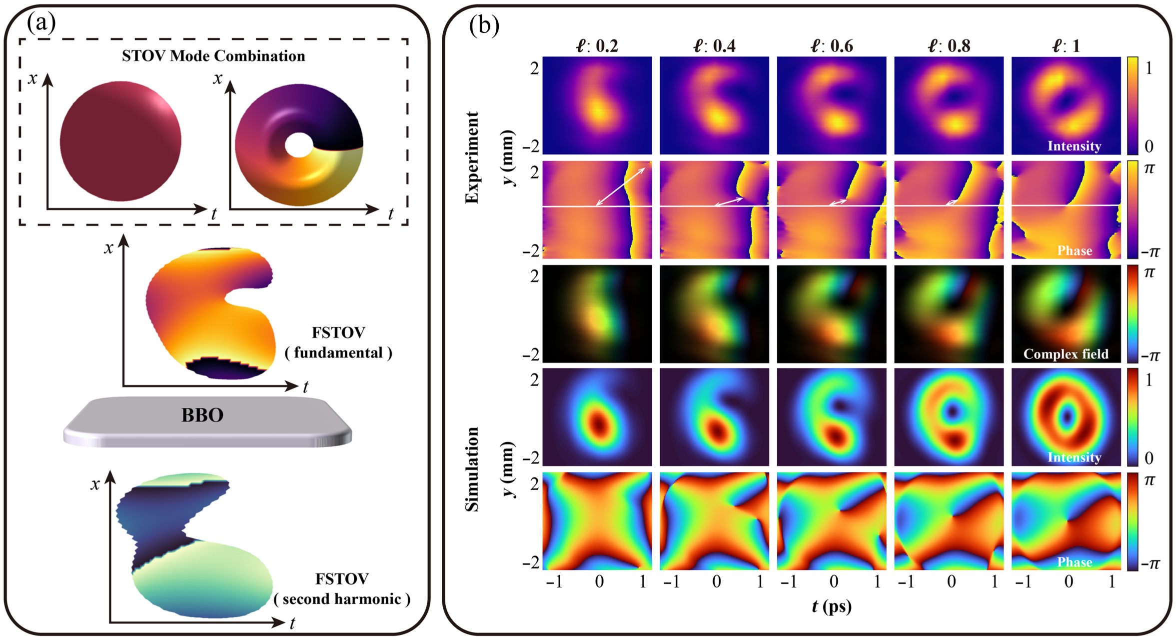

Fig. 1 Concept and evolution of FSTOVs. (a) Schematic diagram illustrating the generation and nonlinear conversion of an FSTOV. The FSTOV is formed by the coherent superposition of two adjacent integer-order STOV modes, resulting in an open-ring intensity profile and a radial phase discontinuity. When passing through a BBO crystal, the FSTOV produces a second-harmonic field with globally doubled phase and locally replicated singularities. (b) Experimental and simulated spatiotemporal intensity and phase distributions for fractional topological charges from $\ell = 0.2$ to 1.0, showing a continuous evolution from an open-gap arc shape to a closed ring, corresponding to the gap-healing and inward-migration dynamics.

closure and introduces a well-defined reference direction, making the initial phase angle ϕ_0 (the gap orientation) an intrinsic degree of freedom that directly shapes the field structure. Here, ϕ_0 denotes the azimuthal position of the branch cut, i.e., the angular location of the phase discontinuity where the optical phase undergoes a non-2π jump. This angle specifies the orientation of the gap in the transverse intensity profile and serves as a global phase reference that would otherwise be undefined in an integer-order vortex. As a result, ϕ_0 parametrizes the broken rotational symmetry and uniquely determines how the fractional circulation is embedded in the spatiotemporal field. Experimentally, ϕ_0 is tuned by rotating the fractional vortex phase mask on the SLM. As shown in Fig. 2, rotating the mask by π reverses the orientation of the phase gap, and the resulting field distributions are related by a 180 deg rotation while preserving the global envelope. This controllable phase offset provides a new encoding channel for multidimensional light-field control (Sec. 2 in the Supplementary Material).

The handedness of the field is determined by the sign of the topological charge. For $\ell > 0$, the phase gradient and local energy flow rotate clockwise on the space–time plane, whereas reversing the sign of ℓ inverts both. As illustrated in Fig. 2, FSTOVs with opposite topological charge exhibit mirror-symmetric phase and momentum-flow patterns while maintaining nearly identical intensity distributions. This independence between orientation and chirality reveals that FSTOVs support two distinct, controllable degrees of freedom—one governing global alignment and the other defining the sense of spatiotemporal rotation.

2.3 Second-Harmonic Generation and Topological Evolution of FSTOVs

To investigate the transfer of OAM in nonlinear frequency conversion, we analyzed the phase and topological evolution of an FSTOV during the second harmonic (SH). Under ideal conditions with perfect phase matching, negligible group-velocity mismatch (GVM, characterized by the parameter η), and dispersion, the SH field can be expressed as

$$E_{\mathrm{SH}}(x,t) \propto [E_{\mathrm{FD}}(x,t)]^2. \tag{3}$$

Here, E_{SH} denotes the ideal second-harmonic field, whereas E_{FD} represents the incident fundamental driving field. If the fundamental FSTOV carries a topological charge ℓ, the SH field ideally acquires a doubled charge of 2ℓ. For instance, when $\ell = 1.5$, the fundamental beam exhibits a dark core and an open-edge singularity, whereas the SH field shows a helical phase with $2\ell = 3$. As shown in Fig. 3(a), the singularities of both orders overlap under ideal conditions, forming a quadratic phase–intensity mapping with preserved topology.

In realistic ultrafast SHG, GVM and dispersion inevitably disturb this ideal mapping. Although dispersion effects exist, our comparative simulations demonstrate that for the thin crystal used (0.05 mm), the topological dynamics are dominated by temporal walk-off induced by GVM, rather than group velocity dispersion (GVD). As verified in Sec. 3 of the Supplementary Material, a control simulation of pure linear propagation (incorporating GVD and diffraction) shows that phase singularities

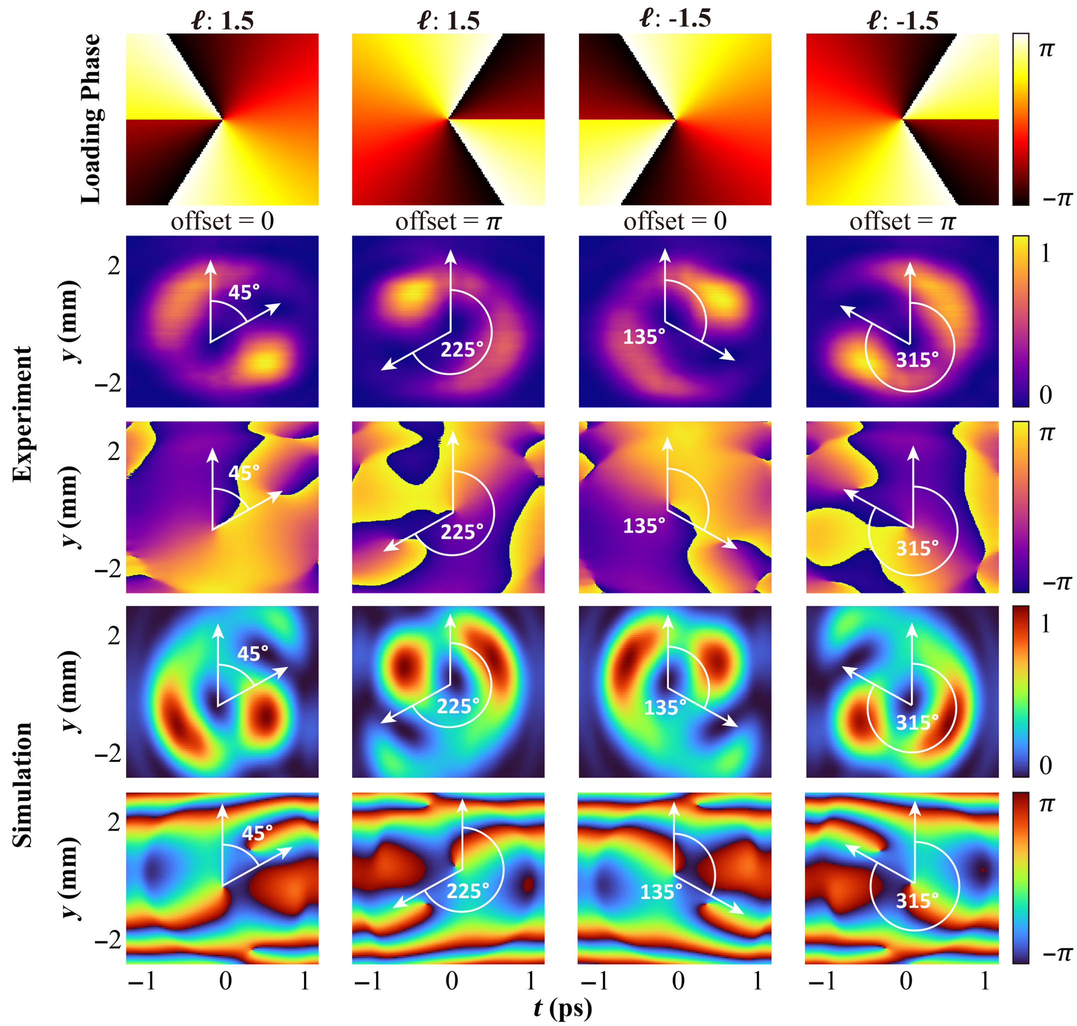

Fig. 2 Influence of initial phase and topological chirality on FSTOVs. The first row shows the applied vortex phase masks with different initial phase orientations. The second and third rows present the corresponding experimental intensity and phase distributions, whereas the fourth and fifth rows display the simulated results under the same conditions. The comparison demonstrates how the initial phase orientation and the sign of the topological charge determine the field's spatial orientation and chirality.

remain largely intact with only minor splitting, consistent with recent theoretical models for SHG of STOVs.[33] Incorporating spatiotemporal GVM coupling into our model and performing full-wave simulations show that the global phase structure remains doubled, but each singularity in the fundamental field splits into a mirror-symmetric pair in the SH field. This splitting originates from GVM-induced temporal and spatial offsets between the pulses, which act as spatiotemporal astigmatism and prevent the complete overlap of phase zeros. As shown in Fig. 3(b), the local canonical momentum density,

$$\mathbf{P}(x,t) \propto |E(x,t)|^2 \nabla \Phi(x,t), \tag{4}$$

reveals this evolution. The originally symmetric circulation of the fundamental beam is stretched into two subsidiary vortices, and the single-edge discontinuity divides into parallel phase-jump surfaces with distinct momentum flows. This redistribution of local momentum generates multiple SHG hotspots and produces a multimode output spectrum shifted toward components with lower OAM (Sec. 3 in the Supplementary Material).

2.4 Systematic Comparison of FSTOVs with Anomalous Topological Conservation

Building on the singularity splitting mechanism revealed above, we systematically examined how FSTOVs evolve across a continuous range of topological charges during SHG. Figure 4 presents the measured temporal intensity and phase distributions of both the fundamental and harmonic fields, confirming the progressive reconstruction of spatiotemporal topology. For small ℓ, the SH field retains the arc-shaped envelope of the fundamental beam but exhibits clear phase doubling, where the single branch cut replicates into two parallel discontinuities. As ℓ increases, the outer-edge singularity bifurcates into a pair in the SH field, demonstrating the onset of singularity multiplication predicted by the model. When ℓ approaches unity, the open intensity pattern gradually closes into a near-complete ring, and

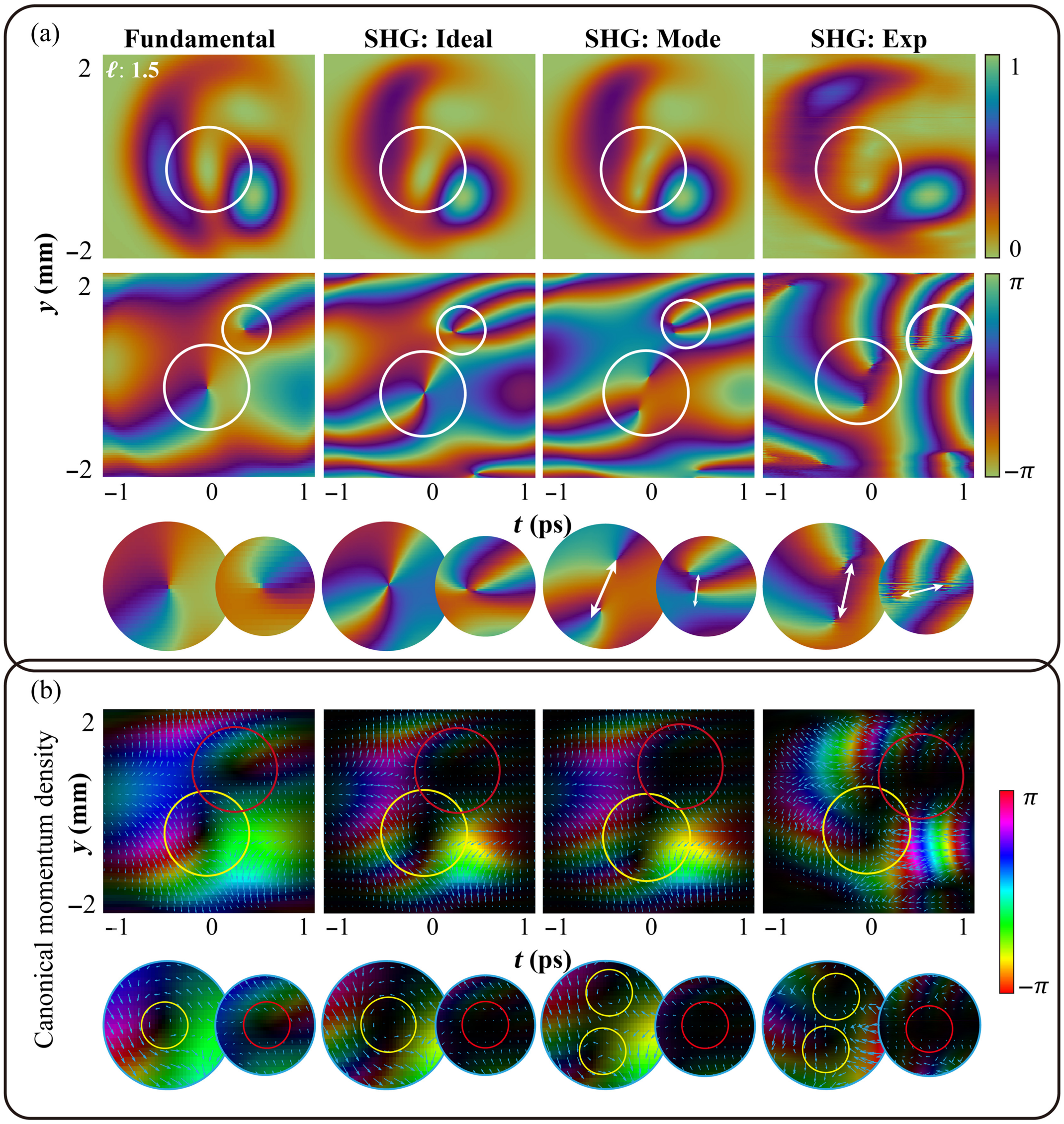

Fig. 3 Second-harmonic generation of an $\ell = 1.5$ FSTOV under different conditions. (a) Intensity and phase distributions of the fundamental field (left column) compared with the second-harmonic (SH) fields obtained under ideal conditions, GVM-coupled theoretical modeling, and experimental measurement. The transition from ideal phase doubling to spatiotemporally induced singularity splitting highlights the deviation from the conventional 2ℓ expectation of angular momentum conservation. (b) Local canonical momentum density of the fundamental field and the SH fields under the three corresponding conditions, showing how GVM and dispersion reshape the energy flow and induce local topological reconstruction.

the doubled singularities move toward the beam center, providing direct evidence of a nonlinear topological transition from an open to a closed configuration.

For $\ell > 1$, the same evolution rule continues, as shown in Fig. 4(b). The fundamental field contains both a central and a secondary edge singularity, and the SH field reproduces each with doubled charge and consistent spatial alignment. With increasing ℓ, the secondary defect moves inward, whereas the overall energy-flow topology remains preserved. This continuous evolution across fractional and integer regimes establishes a unified nonlinear topological law for FSTOVs, characterized by global phase doubling and local singularity replication. Together with the GVM-coupled model in Fig. 3, these observations provide a coherent understanding of how nonlinearity reorganizes fractional topological order into structured harmonic fields, linking linear evolution to nonlinear topological reconstruction. Furthermore, quantitative modal decomposition based on numerical simulations confirms that despite the spectral broadening induced by propagation effects, the global average OAM rigorously follows the frequency-doubling law across the entire fractional domain. We also quantitatively verified the global conservation law by integrating the canonical momentum density of the experimentally reconstructed fields. The results confirm that despite the local redistribution of singularities, the total transverse OAM strictly follows the 2ℓ scaling rule (Sec. 4 in the Supplementary Material).

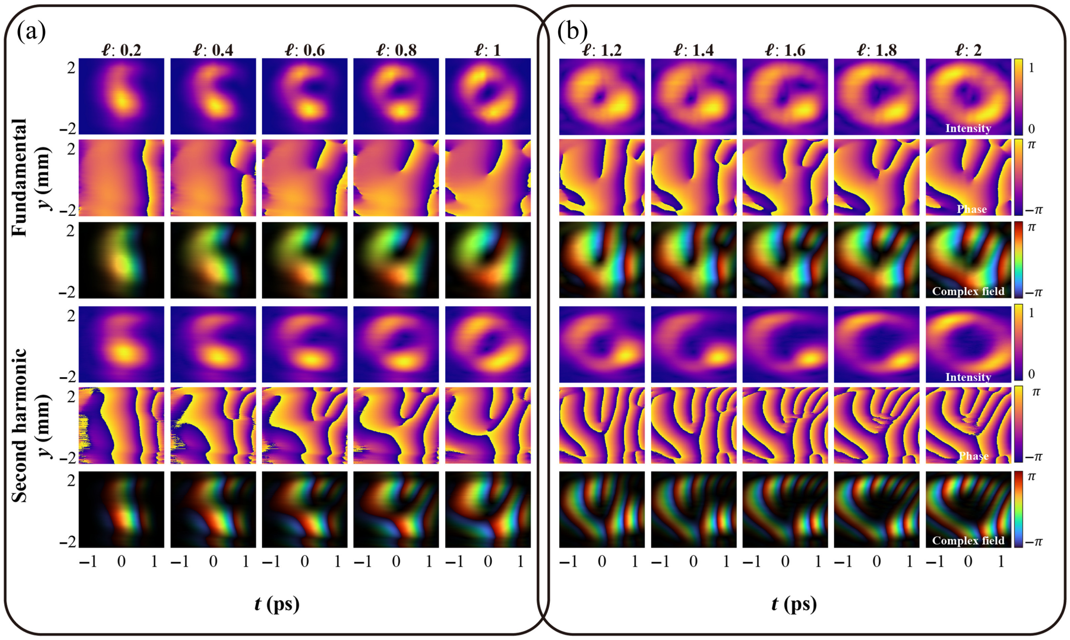

Fig. 4 Experimental comparison between fundamental and second-harmonic FSTOVs. (a) Evolution of FSTOVs as the topological charge ℓ increases from 0.2 to 1.0. (b) Evolution for $\ell > 1.0$ up to 2.0. The upper three rows show the temporal intensity and phase distributions of the fundamental FSTOVs, whereas the lower rows present the corresponding second-harmonic (SHG) results. Both theory and experiment exhibit consistent evolution in intensity closure, singularity migration, and topological reconstruction, confirming the nonlinear coupling of global phase doubling with local singularity multiplication across different ℓ values.

3 Discussion and Conclusion

FSTOVs reveal a higher-order topological complexity of light in the space–time domain. Unlike integer-order STOVs, with phase winds in closed 2π cycles, FSTOVs possess noninteger topological charges that break global phase closure and introduce branch-like discontinuities and directional gaps. These features endow the field with well-defined degrees of freedom for orientation and chirality. Through combined theoretical analysis and experimental observation, we have shown that FSTOVs follow a clear trajectory of topological reconstruction: as the fractional charge continuously increases toward an integer, the field undergoes a dynamic gap-healing and inward-migration process, eventually restoring rotational symmetry and full 2π phase closure. The fractional states can be described as coherent superpositions of adjacent integer modes, where the relative modal weights determine the singularity position and intensity distribution. This framework quantitatively explains the continuous topological transition of light in the spatiotemporal domain. FSTOVs also introduce additional geometric degrees of freedom. The initial phase orientation ϕ_0 serves as an independent, controllable encoding dimension, whereas the sign of ℓ determines the direction of energy circulation and hence the field's handedness. The ability to program these parameters makes FSTOVs promising carriers for high-dimensional light-field modulation and topological information multiplexing.

In nonlinear interactions, FSTOVs display topological evolution that deviates from the conventional 2ℓ scaling expected from angular momentum conservation. Under ideal conditions, their SHG follows a direct mapping of phase doubling and intensity squaring. In realistic ultrafast processes, however, GVM introduces spatiotemporal coupling that splits each fundamental singularity into a pair of mirror-image defects, producing local topological duplication and reorganization. Experiments confirm this phase-doubling and singularity-replication law: regardless of whether ℓ is below or above unity, the SHG field preserves global topological charge while undergoing controllable local restructuring. This coexistence of global conservation and local reconstruction establishes a new paradigm of nonlinear topological mapping.

Overall, the nonlinear response of FSTOVs provides a new route for understanding the interplay between spatiotemporal coupling and topological evolution.[7,34,35] FSTOVs represent a class of nontrivial spatiotemporal topological states with dynamics that are governed by the competition between coherent superposition and nonlinear transformation. Their tunable singularity structures and chirality control open pathways for high-dimensional information transfer,[36–39] ultrafast topological photonics,[40–42] and even open previously inaccessible regimes of light–matter interaction.[11,42,43] Extending this framework to higher-order harmonic generation, strong-field electron dynamics, and topological light–matter interactions could deepen our understanding of the topological dimensions inherent in light–matter coupling.[44]

4 Appendix: Materials and Methods

FSTOVs were generated using a folded $4f$ spatiotemporal pulse-shaping system (Fig. S5 in the Supplementary Material). The driving source was a Yb-based femtosecond laser centered at 1030 nm, with a spectral bandwidth of 10 nm, a pulse duration of 300 fs (FWHM), a repetition rate of 10 kHz, and an average power of 1 W. The beam was divided into two paths. One path was directed into a spatiotemporal pulse shaper composed of a diffraction grating (1200 lines/mm), a cylindrical lens ($f = 200$ mm), and a phase-only spatial light modulator (SLM) placed at the Fourier plane of the $4f$ system. The SLM imposed a fractional-order helical phase $\exp(i\ell\phi)$ across the spatial–frequency spectrum of the pulse, where the topological charge ℓ was continuously tunable from 0 to 1 and beyond. After inverse Fourier transformation, the phase modulation was mapped into the temporal domain, producing an FSTOV pulse at the output.

The second path provided a reference Gaussian pulse. The FSTOV and reference beams were combined collinearly, and their interference fringes were recorded to retrieve the intensity and phase of the FSTOV. This configuration enabled continuous tuning of ℓ and direct observation of its topological evolution, including gap closure and singularity migration during the transition from fractional to integer states. In our measurements, the uncertainty in extracting singularity positions was primarily influenced by the beam pointing stability of the driving laser, which led to slight fluctuations in the interference fringe contrast used for phase retrieval. Importantly, despite these minor fluctuations, the overall topological structure and the evolution trajectory of the FSTOVs remained highly stable and repeatable.

To investigate nonlinear topological behavior, identical type-I β-BaB_2O_4 (BBO) crystals of 0.05 mm thickness were inserted into both the FSTOV and reference paths, with matched positions and orientations to ensure equal optical path and propagation time. This specific thickness was selected to distinctly highlight the GVM-induced topological evolution, whereas the dependence of these effects on crystal thickness was investigated numerically (see Sec. 3 of the Supplementary Material). Specifically, corresponding simulations utilized coupled-wave equations with parameters strictly matching the experimental conditions: a fundamental wavelength of 1030 nm, a second-harmonic at 515 nm, and a calculated GVM of $\eta \approx 94$ fs/mm. GVD was neglected, given the short interaction length, and perfect phase matching ($\Delta k = 0$) was assumed.[33] Detailed model parameters are listed in Table S1 in the Supplementary Material. Each arm generated a second-harmonic (SHG) beam at 515 nm, and the two SHG pulses were subsequently recombined for interference measurement. This symmetric configuration maintained phase stability and allowed retrieval of the spatiotemporal intensity and phase of the FSTOV's second harmonic. The results revealed anomalous topological conservation, where global phase doubling coexisted with local singularity multiplication and reorganization—demonstrating a nonlinear topological reconstruction unique to FSTOVs.

Disclosures

The authors declare no competing interests.

Code and Data Availability

The code and data that support the findings of this study are available from the corresponding author upon reasonable request.

Author Contributions

D.L. and G.F. proposed the original idea and initiated this project. X.Z. completed the theory and simulations. D.L. designed and performed the experiments. D.L. and X.Z. both analyzed the data. D.L., X.Z., G.F., and Q.Z. prepared the paper. All authors contributed to the discussion and writing of the paper.

Acknowledgments

This work was supported by the National Key R&D Program of China (Grant No. 2025YFF0515101 [Q.Z.]), the National Natural Science Foundation of China (Grant Nos. 12374318 [G.F.], 62535013) [Q.Z.], and 12434012 [Q.Z.]), the Science and Technology Commission of Shanghai Municipality (Grant No. 24JD1402600 [Q.Z.]), and the Key Project of Westlake Institute for Optoelectronics (Grant No. 2023GD007 [Q.Z.]).

References

1. L. Allen et al., "Orbital angular momentum of light and the transformation of Laguerre–Gaussian laser modes," *Phys. Rev. A* **45**(11), 8185, 8189 (1992).
2. L. Paterson et al., "Controlled rotation of optically trapped microscopic particles," *Science* **292**(5518), 912–914 (2001).
3. D. L. Whitaker and J. Edwards, "Sphagnum moss disperses spores with vortex rings," *Science* **329**(5990), 406–406 (2010).
4. N. Bozinovic et al., "Terabit-scale orbital angular momentum mode division multiplexing in fibers," *Science* **340**(6140), 1545–1548 (2013).
5. Y. Shen et al., "Optical vortices 30 years on: OAM manipulation from topological charge to multiple singularities," *Light Sci. Appl.* **8**(1), 90 (2019).
6. A. Forbes, M. De Oliveira, and M. R. Dennis, "Structured light," *Nat. Photonics* **15**(4), 253–262 (2021).
7. J. Ni et al., "Multidimensional phase singularities in nanophotonics," *Science* **374**(6566), eabj0039 (2021).
8. A. M. Yao and M. J. Padgett, "Orbital angular momentum: origins, behavior and applications," *Adv. Opt. Photonics* **3**(2), 161–204 (2011).
9. G. Molina-Terriza, J. P. Torres, and L. Torner, "Twisted photons," *Nat. Phys.* **3**(5), 305–310 (2007).
10. J. Wang et al., "Terabit free-space data transmission employing orbital angular momentum multiplexing," *Nat. Photonics* **6**(7), 488–496 (2012).
11. L. Rego et al., "Generation of extreme-ultraviolet beams with time-varying orbital angular momentum," *Science* **364**(6447), eaaw9486 (2019).
12. A. Chong et al., "Generation of spatiotemporal optical vortices with controllable transverse orbital angular momentum," *Nat. Photonics* **14**(6), 350–354 (2020).
13. C. Wan et al., "Toroidal vortices of light," *Nat. Photonics* **16**(7), 519–522 (2022).
14. S. Huang et al., "Spatiotemporal vortex strings," *Sci. Adv.* **10**(19), eadn6206 (2024).
15. N. Jhajj et al., "Spatiotemporal optical vortices," *Phys. Rev. X* **6**(3), 031037 (2016).
16. Q. Cao et al., "Propagation of transverse photonic orbital angular momentum through few-mode fiber," *Adv. Photonics* **5**(3), 036002 (2023).
17. S. Hancock, S. Zahedpour, and H. Milchberg, "Mode structure and orbital angular momentum of spatiotemporal optical vortex pulses," *Phys. Rev. Lett.* **127**(19), 193901 (2021).
18. C. Wan, A. Chong, and Q. Zhan, "Optical spatiotemporal vortices," *eLight* **3**(1), 11 (2023).
19. Y. Liu et al., "Integrated vortex soliton microcombs," *Nat. Photonics* **18**(6), 632–637 (2024).
20. Y. Fang, S. Lu, and Y. Liu, "Controlling photon transverse orbital angular momentum in high harmonic generation," *Phys. Rev. Lett.* **127**(27), 273901 (2021).

21. G. Gui et al., "Second-harmonic generation and the conservation of spatiotemporal orbital angular momentum of light," *Nat. Photonics* **15**(8), 608–613 (2021).
22. R. Martín-Hernández et al., "Extreme-ultraviolet spatiotemporal vortices via high harmonic generation," *Nat. Photonics* **19**(8), 817–824 (2025).
23. R. Ni et al., "Topological charge transfer in frequency doubling of fractional orbital angular momentum state," *Appl. Phys. Lett.* **109**(15), 151103 (2016).
24. C. Alexeyev, Y. A. Egorov, and A. Volyar, "Mutual transformations of fractional-order and integer-order optical vortices," *Phys. Rev. A* **96**(6), 063807 (2017).
25. B. Berger et al., "Spectroscopy of fractional orbital angular momentum states," *Opt. Express* **26**(24), 32248–32258 (2018).
26. K. Huang et al., "Spiniform phase-encoded metagratings entangling arbitrary rational-order orbital angular momentum," *Light Sci. Appl.* **7**(3), 17156 (2018).
27. Z. Zhang et al., "Ultrafast control of fractional orbital angular momentum of microlaser emissions," *Light Sci. Appl.* **9**(1), 179 (2020).
28. G. Jing et al., "Recognizing fractional orbital angular momentum using feed forward neural network," *Results Phys.* **28**, 104619 (2021).
29. J. B. Götte et al., "Light beams with fractional orbital angular momentum and their vortex structure," *Opt. Express* **16**(2), 993–1006 (2008).
30. A. Turpin et al., "Extreme ultraviolet fractional orbital angular momentum beams from high harmonic generation," *Sci. Rep.* **7**(1), 43888 (2017).
31. H. Zhang et al., "Review on fractional vortex beam," *Nanophotonics* **11**(2), 241–273 (2022).
32. Z. Liu et al., "Superhigh-resolution recognition of optical vortex modes assisted by a deep-learning method," *Phys. Rev. Lett.* **123**(18), 183902 (2019).
33. X. Gao et al., "Space–time singularity dynamics for second harmonic spatiotemporal optical vortices," *Adv. Photonics Nexus* **4**(3), 036003 (2025).
34. D. Gauthier et al., "Tunable orbital angular momentum in high-harmonic generation," *Nat. Commun.* **8**(1), 14971 (2017).
35. H. E. Kondakci and A. F. Abouraddy, "Optical space-time wave packets having arbitrary group velocities in free space," *Nat. Commun.* **10**(1), 929 (2019).
36. H. Ren et al., "On-chip noninterference angular momentum multiplexing of broadband light," *Science* **352**(6287), 805–809 (2016).
37. L. Gong et al., "Optical orbital-angular-momentum-multiplexed data transmission under high scattering," *Light Sci. Appl.* **8**(1), 27 (2019).
38. Z. Ji et al., "Photocurrent detection of the orbital angular momentum of light," *Science* **368**(6492), 763–767 (2020).
39. X. Fang et al., "Orbital angular momentum-mediated machine learning for high-accuracy mode-feature encoding," *Light Sci. Appl.* **13**(1), 49 (2024).
40. D. Giovannini et al., "Spatially structured photons that travel in free space slower than the speed of light," *Science* **347**(6224), 857–860 (2015).
41. R. C. Devlin et al., "Arbitrary spin-to–orbital angular momentum conversion of light," *Science* **358**(6365), 896–901 (2017).
42. L. Chen et al., "Synthesizing ultrafast optical pulses with arbitrary spatiotemporal control," *Sci. Adv.* **8**(43), eabq8314 (2022).
43. L. Rego et al., "Necklace-structured high-harmonic generation for low-divergence, soft X-ray harmonic combs with tunable line spacing," *Sci. Adv.* **8**(5), eabj7380 (2022).
44. K. M. Dorney et al., "Controlling the polarization and vortex charge of attosecond high-harmonic beams via simultaneous spin–orbit momentum conservation," *Nat. Photonics* **13**(2), 123–130 (2019).
45. K. Y. Bliokh et al., "Spin–orbit interactions of light," *Nat. Photonics* **9**(12), 796–808 (2015).
46. J. Wang, M. Zepf, and S. Rykovanov, "Intense attosecond pulses carrying orbital angular momentum using laser plasma interactions," *Nat. Commun.* **10**(1), 5554 (2019).
47. I. Meglinski et al., "Phase preservation of orbital angular momentum of light in multiple scattering environment," *Light Sci. Appl.* **13**(1), 214 (2024).
48. G. Gui et al., "Second-harmonic generation and the conservation of spatiotemporal orbital angular momentum of light," *Nat. Photonics* **15**(8), 608–613 (2021).
49. M. W. Hyde, IV and M. A. Porras, "Propagation of spatiotemporal optical vortex beams in linear, second-order dispersive media," *Phys. Rev. A* **108**(1), 013519 (2023).

Guangyu Fan received his PhD in the Department of Photonics at Vienna University of Technology. He is currently a professor at the University of Shanghai for Science and Technology (USST). His research interests include novel spatiotemporal optical fields, ultrafast optics, and nonlinear optics.

Qiwen Zhan received his PhD in electrical and computer engineering from the University of Minnesota. He is currently the principal investigator of the Nano-photonics Research Group at USST.

Biographies of the other authors are not available.